Atmos. Chem. Phys. Discuss., 14, 3459–3497, 2014
www.atmos-chem-phys-discuss.net/14/3459/2014/
doi:10.5194/acpd-14-3459-2014

Atmospheric Chemistry and Physics Discussions

Aerosol hygroscopicity parameter derived from the light scattering enhancement factor measurements in the North China Plain

J. Chen[1], C. S. Zhao[1], N. Ma[1,*], and P. Yan[2]

[1]Department of Atmospheric and Oceanic Sciences, School of Physics, Peking University, Beijing 100871, China
[2]Meteorological Observation Centre, China Meteorological Administration, Beijing 100871, China
[*]now at: Leibniz Institute for Tropospheric Research, Permoserstr. 15, 04318 Leipzig, Germany

Received: 18 December 2013 – Accepted: 21 January 2014 – Published: 6 February 2014

Correspondence to: C. S. Zhao (zcs@pku.edu.cn)

Published by Copernicus Publications on behalf of the European Geosciences Union.

Abstract

The relative humidity (RH) dependence of aerosol light scattering is an essential parameter for accurate estimation of the direct radiative forcing induced by aerosol particles. On account of the insufficient information of aerosol hygroscopicity in climate models, more details of the parameterized hygroscopic growth factors are urgently required. In this paper, a retrieval method to calculate the aerosol hygroscopicity parameter, κ, is proposed based on the in situ measured aerosol light scattering enhancement factor, namely f(RH), and particle number size distribution (PNSD) obtained from the HaChi (Haze in China) campaign. Measurements show that f(RH) sharply increases with the ascending RH, and the variation range of f(RH) is much wider at higher RH. Sensitivity study reveals that the f(RH) is more sensitive to the aerosol hygroscopicity than PNSD. f(RH) for polluted cases is distinctly higher than that for clean periods at a specific RH. The derived equivalent κ, combining with the PNSD measurements, is applied in the prediction of the CCN number concentration. Comparison between the predicted CCN number concentration with the derived equivalent κ and the measured ones agrees well, especially at high supersaturations. The proposed calculation algorithm of κ with the f(RH) measurements is demonstrated to be reasonable and can be widely used.

1 Introduction

Atmospheric aerosols have exhibited great contribution to the uncertainties when predicting climate radiative forcing (IPCC, 2007). The aerosol optical property is a crucial input parameter for accurate estimation of the direct radiative forcing caused by aerosols in climate models. Covert et al. (1972) indicated that aerosol hygroscopicity can affect their optical properties via changing the particle size and refractive index, and hence influence the climatic and environmental effects of aerosols. As a result, the relative humidity (RH) dependence of aerosol optical properties, e.g., light

ACPD
14, 3459–3497, 2014

scattering, is a key factor to the estimation of aerosol radiative forcing (Charlson et al., 1992; Schwartz, 1996). For better simulation and prediction of radiative transfer, along with aerosol relevant physical processes, parameterized forms of aerosol hygroscopic growth factors are usually required in General Circulation Models (GCMs). However, detailed information of aerosol hygroscopicity is always insufficient for the model input of GCMs. This therefore calls for more comprehensive description and corresponding parameterization of aerosol hygroscopicity.

Aerosol optical growth factor (denoted by $f(\mathrm{RH})$) is one of the physical parameters commonly applied to describe aerosol hygroscopicity. It's usually defined as the ratio of aerosol light scattering coefficients at a given RH ($\sigma_{\mathrm{sc}}(\mathrm{RH})$) and dry condition ($\sigma_{\mathrm{sc,\,dry}}$), namely, $f(\mathrm{RH}) = \sigma_{\mathrm{sc}}(\mathrm{RH})/\sigma_{\mathrm{sc,\,dry}}$. Numerous studies have demonstrated that the parameterized $f(\mathrm{RH})$ can be generally expressed as an exponential function of RH (Covert et al., 1972; Fitzgerald et al., 1982; Carrico et al., 1998, 2000, 2003; Kotchenruther et al., 1999; Hegg et al., 2002; Randriamiarisoa et al., 2006; Cheng et al., 2008; Pan et al., 2009; Fierz-Schmidhauser et al., 2010a–c; Zieger et al., 2010, 2013). It should be noted that, differ from the size-resolved aerosol diameter growth factor ($g(\mathrm{RH})$), the aerosol light scattering enhancement factor stands for the overall hygroscopicity of the aerosol population, and jointly determined by the particle number size distribution (PNSD), hygroscopicity, and aerosol optical properties.

In the late 1970s, Pilat and Charlson (1966) had attempted to measure the aerosol light scattering enhancement factor with a tandem integrating nephelometer. In the following studies, Covert et al. (1972) introduced a measuring method to determine the $f(\mathrm{RH})$ at a set RH value with a humidified integrating nephelometer. Up to now, the instruments based on the principle of humidified nephelometer measurement have been improved (Fierz-Schmidhauser et al., 2010a–c). To be specific, with adding a set of PID (Proportional-Integral-Derivative) controller to the humidified nephelometer system, the modified instrument can realize a quick response to the set RH, and can also achieve the automatic regulation of the RH variation.

ACPD
14, 3459–3497, 2014

With the above-mentioned hygroscopicity measurement technologies, numerous f(RH)-related observations have been successively conducted worldwidely. In the studies of Malm et al. (2001, 2003), results showed that aerosol can still take up water at relatively low RH. Nessler et al. (2005) found that f(RH) is highly dependent on the mean particle diameter at a constant RH. By measuring and modeling f(RH) for various aerosol types, comparison results reveal that the f(RH) for marine aerosols (Carrico et al., 1998, 2000, 2003; McInnes et al., 1998; Gasso et al., 2000; Wang et al., 2007; Fierz-Schmidhauser et al., 2010b; Zieger et al., 2010) is generally higher than that for either urban (Fitzgerald et al., 1982; McInnes et al., 1998; Yan et al., 2009; Zieger et al., 2011) or continental aerosols (Sheridan et al., 2001; Fierz-Schmidhauser et al., 2010c; Zieger et al., 2012, 2013). The f(RH) for mineral dust and freshly emitted biomass burning aerosols is significantly lower (Kotchenruther and Hobbs, 1998; Li-Jones et al., 1998; Carrico et al., 2003; Kim et al., 2006; Fierz-Schmidhauser et al., 2010a; Zieger et al., 2012). It should be noted that the f(RH) for marine aerosols would show a decrease with strong anthropogenic influence (McInnes et al., 1998; Gasso et al., 2000; Wang et al., 2007; Fierz-Schmidhauser et al., 2010b; Zieger et al., 2010).

In the current research on aerosol hygroscopic and activation properties, one essential mission is to reliably predict the number concentration of cloud condensation nuclei (CCN). It's known that, at a given supersaturation, the aerosol activation ability is primarily determined by the particle size and aerosol hygroscopicity (Seinfeld and Pandis, 1998). The online continuous observations of aerosol size can be easily achieved with some commercial instruments. However, the direct measurements of aerosol hygroscopicity are relatively tougher a lot. In this work, we attempt to derive the hygroscopicity parameter, κ, with the measured f(RH). Analogous work had been reported by Ervens et al. (2007). In the proposed approach, the assumption that the aerosol was just consisted of a soluble fraction of ammonium sulfate and an insoluble component was applied. By varying the insoluble mass fraction, with modulating the comparison results between the measured and calculated f(RH) at a specific RH to the minimum deviation, the aerosol hygroscopicity parameter can be obtained. It therefore provides

ACPD
14, 3459–3497, 2014

a possible way for the prediction of aerosol activation property, hence building a bridge for the estimation of CCN number concentration with the measured PNSDs. It should be convinced that the retrieval algorithm of κ with the f(RH) measurements is of significant utility and applicability.

Recently, with the rapid economic growth, along with the sharp aggravation of the industrialization and urbanization processes, most megacities in the north China plain (NCP) have inevitably experienced severe aerosol pollution. Accompanied aerosol pollution episodes, as well as the aerosol-related environmental and health effects, have aroused great public concern. Considering the unique physical and chemical characteristics of aerosol particles in this region, researches on aerosol hygroscopicity are thus of special necessity. Previous studies indicated that aerosols in the highly polluted NCP are of strong hygroscopicity (Liu et al., 2011). Consequently, it would result in immense impact on aerosol optical and activation properties (Deng et al., 2011; Chen et al., 2012). Nevertheless, due to the limitation of measurement technologies, it's relatively difficult to directly measure the aerosol hygroscopicity, and hence the corresponding research results are insufficient in this area (Massling et al., 2009; Meier et al., 2009). On account of the observation of aerosol light scattering enhancement factors is more feasible in practical application, many measurements of f(RH) have been carried out in the NCP; while relevant studies on f(RH) in the northern NCP are relatively scarce (Pan et al., 2009; Yan et al., 2009). For better estimation of the radiative forcing by aerosols in the NCP, a comprehensive description of aerosol hygroscopicity and parameterized hygroscopic growth factors are urgently needed in climate models.

In this study, 20 day well-maintained f(RH) observations, obtained from the Haze in China (HaChi) field campaign conducted in Wuqing, Tianjin, were analyzed. In Sect. 3.1, the statistical characteristics of f(RH) in the northern NCP, along with their variations under different pollution levels, were discussed. The followed Sects. 3.2 and 3.3 presented the sensitivity studies on dominating influence factors of f(RH) and the parameterization results of f(RH), respectively. A new algorithm for deriving aerosol hygroscopicity parameter was introduced in Sect. 3.4. An application of the retrieved κ

ACPD
14, 3459–3497, 2014

in the prediction of the CCN number concentration (N_{CCN}), along with the comparison study of N_{CCN} between the calculated and in situ measured values, was performed in Sect. 3.5. These results are of great reference value to the relevant model simulations of aerosol particles in the northern NCP.

2 Experiment and instrumentation

The Wuqing site (39°23′ N, 117°01′ E, 6 m a.s.l.) is a suburban observation station in the NCP. It's situated in between the megacities Beijing and Tianjin. Wuqing can highly represent the regional aerosol pollution in the northern NCP. More information of the site description can be found in Ran et al. (2011) and Liu et al. (2011). A fog and haze experiment of the HaChi project was carried out at Wuqing from the end of October 2009 to late January 2010. The aim of the campaign is to obtain some more insight of the physical and chemical characteristics of pollution aerosols, as well as the difference of aerosol optical properties between fog and haze, hence serving as reference criteria for distinguishing fog from haze.

During the entire experiment, ground-level aerosol size distribution, optical and activation properties, visibility and meteorological parameters were measured. Specifically, the PNSD observations measured by a scanning mobility particle sizer (SMPS) were only in the submicron size range (14–736 nm), with the time resolution of 5 min. A continuous-flow dual CCN counter (CCN-200, DMT, USA) (Roberts and Nenes, 2005; Lance et al., 2006) was utilized to measure the aerosol activation properties at five set supersaturations (nominally 0.07, 0.10, 0.20, 0.40, and 0.80 %). The observations were recorded every 30 min, and details can be obtained in Deng et al. (2011). The continuous f(RH) measurement with a humidification system took place in the duration of 1–20 January 2010. A complete humidification cycle, with both elevated and decreased RH periods, lasted for about two and a half hours. The temporal resolution of the measurements of aerosol light scattering and absorption, visibility, as well as meteorological parameters, was one minute.

ACPD
14, 3459–3497, 2014

As introduced before, the two integrating nephelometers operated in parallel are often applied in the measurement of f(RH). What we used in this work is the integrating nephelometer (TSI Inc., Model 3563) at three wavelengths of 450, 550 and 700 nm, respectively. With no special statement, the wavelength of 550 nm is chosen for discussion in this study. In the humidification system, one reference nephelometer is used to measure the aerosol light scattering coefficient at dry conditions (usually defined as RH < 40 %), shortly called as "Dry-NEPH"; the other one, correspondingly named as "Humi-NEPH", is operated in humidified conditions, hence the aerosol light scattering at a given RH is determined. The humidifier in the Humi-NEPH mainly consists of the following two parts. That is, it comprises a deionized water bath connected in between the inhaled aerosol sample line and the nephelometer, and a water vapor penetrating membrane tube immerged through a heatable metal pipe. The aerosol flow is first exposed to an increasing RH in the humidifier till a maximum RH value has been reached inside the Humi-NEPH, and then dehydrated with the decrease of RH. The given RH, depending on the flow and surrounding temperature conditions, is achieved by controlling of the water temperature inside the water bath. To be specific, with modulating the power of heating equipment, the water temperature is regulated, and in turn controls the water vapor permeated to mix with aerosol sample. Details of the Humi-NEPH can refer to Covert et al. (1972) and Fierz-Schmidhauser et al. (2010c).

Figure 1 illustrates the comparison results of the light scattering coefficients measured with the two nephelometers both at dry conditions of RH below 40 %. It's distinct that the dry σ_{sc} measured with the Humi-NEPH generally agrees well with that measured with the reference Dry-NEPH, with the correlation coefficient higher than 0.99. However, the discrepancy between the two observations would present more significant at higher σ_{sc} conditions. This is probably due to the weak hygroscopic growth of aerosols at low RH. Another possible explanation may be attributed to the drifting electronic signals of Photomultiplier at severe aerosol pollution conditions; in other words, the limitation of instrument itself in high σ_{sc} cases can also result in deviation to the measurement.

ACPD
14, 3459–3497, 2014

3 Results and discussion

In this section, statistical characteristics of the aerosol optical growth factor, along with the simultaneously measured meteorological parameters will be analyzed at first. Then follows the sensitivity study on the predominant factor influencing the variation of $f(\mathrm{RH})$. The parameterized forms of $f(\mathrm{RH})$ under different pollution cases are also presented. In the end, an algorithm for retrieving the aerosol hygroscopicity parameter, κ, with $f(\mathrm{RH})$ measurements is introduced.

3.1 Overview of the measurements

In Fig. 2, the in situ measured $f(\mathrm{RH})$, aerosol optical and meteorological parameters during the experiment are presented. From top to bottom, it orderly shows the time series of the $f(\mathrm{RH})$ measurements at elevated RH, the corresponding RHs inside the Humi-NEPH in ascending RH periods, aerosol light scattering coefficients at 550 nm wavelength (σ_{sc}^{550}) at both dry and humidified conditions, every-minute visibility (VIS) and RH observations, along with the wind vectors.

Throughout the observation period, two aerosol pollution episodes can be evidently found in Fig. 2. These processes are highly correlated with meteorological parameters, especially with the wind speed and wind direction. From 1 January to the early morning of 4 January, the prevailing wind is continuous easterly, with the 1 min mean wind speed generally maintaining below 5 $\mathrm{m\,s^{-1}}$. The dry σ_{sc} keeps fluctuating within 500 $\mathrm{Mm^{-1}}$, the region is in slightly polluted situation. Between 4 January and the evening of 5 January, the observation site is witnessed by continuous strong north wind, and the mean wind speed is nearly above 5 $\mathrm{m\,s^{-1}}$. As a result, most of the accumulated air pollutants are swept away, and the corresponding dry σ_{sc} maintains at an extremely low level. However, pollutants start to accumulate at constant low wind speed from 6 January, and the dry σ_{sc} reaches a maximum level in 10 January, approaching to 1500 $\mathrm{Mm^{-1}}$. In the beginning of 11 January, aerosol pollutants are removed by high winds from the north. The clean condition almost lasts till the morning of 16 January. Later on, air

ACPD
14, 3459–3497, 2014

pollutants gradually accumulate in the campaign site when controlled by relatively low wind. The dry σ_{sc} in the period of 17–20 January is always higher than 1000 Mm^{-1}. These pollution accumulation and removal processes are also reflected in the corresponding variation of visibility. With the increase/decrease of aerosol light scattering, visibility would present a very coincident fluctuation. There is a positive correlation between the visibility and σ_{sc}, while the RH and visibility are approximately negatively correlated with each other.

During the f(RH) measurements, 117 valid humidifying cycles are achieved. Generally, the humidifier is capable of increasing the RH from 30 % to 90 %. Nevertheless, the cases of RH lower than 20 % and up to 95 % are occasionally observed, as shown in the corresponding series of RH inside the Humi-NEPH. Overall, the measured f(RH) varies in the range of 1.0–3.0. To the specific characteristics of f(RH) observations, more detailed information can be obtained from the statistical results of f(RH) summarized in Table 1.

Considering the variation of measured dry σ_{sc} during different pollution levels, several typical observation periods are selected to categorize the clean and polluted cases. Specifically, during the periods of DOY4.2–5.6 and DOY11–13.5 (DOY here means the date of the year, e.g., DOY1.5 thus represents 12:00 LT of 1 January, and so on.), the dominating wind is continuous strong northerly, with the wind speed of around 5 $m\,s^{-1}$. The Wuqing site is controlled by the clean air mass from the north regions, and the two periods are consequently chosen as the representative of clean conditions. During DOY7–11 and DOY16–20, the wind speed almost keeps at about 1 $m\,s^{-1}$ level. The campaign site is mainly influenced by the local emissions and pollutants from surrounding areas. As a result, the two time periods are used to characterize the polluted cases.

Table 1 displays the mean and corresponding standard deviation (σ) values of in situ measured f(RH) at specific RHs under different pollution levels. It can be found that f(RH) significantly increases with the ascending RH. To be specific, at 80 % RH, the mean f(RH) values in clean and polluted cases are 1.46 ± 0.15 and

ACPD
14, 3459–3497, 2014

1.58 ± 0.19, respectively; while the corresponding mean f(RH) to the overall average condition is 1.58 ± 0.22, approximating to that of the value during polluted periods. The f(RH = 80 %) measurements presented here are comparable to the results concluded by Pan et al. (2009) at a rural site near Beijing, with the mean f(RH) values of 1.31 ± 0.03 and 1.57 ± 0.02 corresponding to clean and urban pollution episodes, respectively. These values are all much higher than those reported by Yan et al. (2009) for the Shangdianzi background observation station, another rural site of northern China with lower anthropogenic influence.

At RH = 90 %, the mean f(RH) for the entire observation period is 1.90 ± 0.27, while the mean values for both clean and polluted conditions are 1.71 ± 0.26 and 1.93 ± 0.21, respectively. It should be noted that the general mean f(RH = 90 %) is roughly approaching 2.0. From the definition of f(RH), it indicates that the integral light scattering of the aerosol population has nearly doubled with respect to the σ_{sc} at dry conditions. As suggested in previous studies, aerosol light scattering approximately contributes 90 % of the total aerosol light extinction, and this proportion would increase with higher RH (Yuan et al., 2006; Cheng et al., 2008; Chen et al., 2012). In other words, to be simplification, aerosol light extinction at 90 % RH would be enhanced twice as the corresponding value at dry conditions. According to the Kosiemider theory (Seinfeld and Pandis, 1998), there is an empirical negative correlation between the visibility and light extinction. In this sense, the visibility would therefore be degraded to be half of the level at dry conditions. This is of great instructive significance to the low visibility monitoring and forecast for relevant environment departments.

Table 1 also presents the mean f(RH) results corresponding to both clean and polluted cases. The f(RH) for clean periods is distinctly lower than the corresponding value for polluted episodes at each specific RH. In addition, the overall mean f(RH) for the whole observation period is even closer to the mean value for polluted cases, as a result of the longer duration of polluted conditions than that of the clean periods. Similar conclusions can be easily drawn from Fig. 3.

ACPD
14, 3459–3497, 2014

Figure 3 illustrates the corresponding variations of mean f(RH) with RH during the clean, average, and polluted periods. The right panel (Fig. 3b) displays the occurrence frequency distributions of measured f(RH) at four selected RHs. It's apparent that f(RH) presents an approximating exponential variation with the increase of RH. The variation range of the f(RH) observations seems to be wider at higher RH, as evidently indicated by the PDF of f(RH) in Fig. 3b. At a specific RH, the f(RH) for polluted episodes is significantly higher than that for clean cases. In particular, the deviation of f(RH) between those measured under clean and polluted conditions would be more notable at higher RHs.

The error bar, or rather the standard deviation, of the overall mean f(RH) at a given RH presents an increasing trend with the ascending RH. The possible reasons for the variation range of f(RH) at different RHs can be attributed as below. As illustrated by the definition of f(RH), it denotes the ratio of aerosol light scattering at a specific RH to dry scattering coefficient. Hence, the variation of f(RH) is mainly contributed by the variation of σ_{sc} in humidified conditions. According to the theoretical calculation of aerosol optical properties at a fixed wavelength with the Mie model (Mie, 1908; Bohren and Huffman, 1983), the crucial input parameters primarily include the particle size, refractive index, and aerosol size distribution. At ambient environment, aerosol hygroscopic growth can change the particle size and refractive index by taking up water, and this effect would be more significantly presented with the increase of RH. Nevertheless, previous investigations have demonstrated that the aerosol refractive index varies little with the changing RH, hence with slight influence on the aerosol light scattering (Lesins et al., 2002; Cheng et al., 2006). Consequently, the key factors of dominating the variation of f(RH) should be ascribed to the aerosol size distribution and hygroscopicity. In general, at low RH, aerosol hygroscopic growth is not so apparent, leading to the accompanied shift of PNSD also indistinct, and thus induce a relatively narrow variation range of f(RH). While at high RH, the influence of aerosol hygroscopic growth on both of the particle size and PNSD pattern would be much more significant. As a result, it will dramatically affect the variation of f(RH).

ACPD
14, 3459–3497, 2014

Briefly, the f(RH) is determined by both of the PNSD and aerosol hygroscopicity related to the chemical composition. To understand how f(RH) is dependent on the aerosol size distribution and aerosol hygroscopicity, a detailed sensitivity study is needed.

3.2 Factors influencing f(RH)

Detailed procedures of the sensitivity study are as follows: (1) with a fixed PNSD, varying the aerosol hygroscopic growth factors, the f(RH) values corresponding to different water uptake abilities can be theoretically estimated with the Mie model. This illustrates how f(RH) depends on aerosol hygroscopicity. Specifically, a mean PNSD is used in this work. (2) Using a constant aerosol hygroscopicity parameter, κ, while altering the PNSD, the f(RH) corresponding to each PNSD can be derived from the Mie calculation. Here we use the temporal averaged size-resolved hygroscopic growth factors. Correspondingly, this is regarded as the sensitivity test of f(RH) to the aerosol size distribution.

For the consideration of simplifying calculation, the sensitivity study of f(RH) to the aerosol hygroscopicity is based on the assumption that a specific PNSD corresponds to an integral mean κ. By changing the value of the overall mean κ, the mean size-resolved aerosol hygroscopic growth factors corresponding to different water absorption capabilities can be derived with the κ-Köhler theory (Petters and Kreidenweis, 2007). Combined with the fixed PNSD, the variation of f(RH) under different hygroscopic capacities can be estimated with the Mie model.

On account of the integrity and availability of the corresponding data for the sensitivity studies, the in situ measured PNSDs, mean size-resolved hygroscopic growth factors, along with the aerosol optical observations during the HaChi summer campaign are applied in the theoretical calculation of f(RH) with the Mie model. Comprehensive information of the HaChi field campaign and relevant data can be found in previous studies (Liu et al., 2011; Ma et al., 2011; Chen et al., 2012). Results of the sensitivity studies are given in Fig. 4.

ACPD
14, 3459–3497, 2014

The left panel of Fig. 4 shows the equivalent f(RH) derived from the in situ measured dry σ_{sc} and ambient visibilities. With the visibility observations, the ambient light extinction can be obtained by using the Kosiemider theory (Seinfeld and Pandis, 1998). Based on the single scattering albedo induced by the measurements of light scattering and absorption at dry conditions, the ambient σ_{sc} can then be roughly estimated with the light extinction. In this case, the variation of the achieved f(RH) at a specific RH (namely, Δf(RH)) should be caused by the fluctuation of both PNSD and aerosol hygroscopicity.

The middle panel presents the sensitivity study of f(RH) to the aerosol size distribution. The mean size-resolved hygroscopic growth factors are applied in the Mie calculation. As a result, it can be considered as a constant κ to all the measured PNSDs. The Δf(RH) in this condition should be mainly induced by the varying PNSD patterns. However, unlike the highly perturbation of measured f(RH), little variation of Δf(RH) is found in this sensitivity study.

The right panel illustrates the sensitivity results of f(RH) to aerosol hygroscopicity. It can be found that the f(RH) curves are elevated with the increase of the mean κ values. That is, at a selected RH, the higher the mean κ is, the larger the absolute f(RH) value is. It would be more apparently presented at high RH conditions.

Generally, the sensitivity studies demonstrate that, at a specific RH, the f(RH) seems to be more sensitive to the variation of aerosol hygroscopicity. It might be mainly induced by the varying chemical components of aerosol particles. The variation of PNSD patterns can also influence the f(RH), and the effect would be more significant at high RH conditions.

3.3 A parameterization scheme of f(RH)

At low RH, the variation of f(RH) is inconspicuous; while the f(RH) would vary dramatically with the ascending RH under high RH conditions. For better description of the variation of f(RH), the stepwise function is applied to fit the f(RH) measurements. On the basis of previously suggested empirical functions (Carrico et al., 1998, 2000, 2003;

ACPD
14, 3459–3497, 2014

Kotchenruther et al., 1999; Hegg et al., 2002; Randriamiarisoa et al., 2006; Pan et al., 2009), a specific polynomial segment fitting, with the critical RH of 60 %, is chosen to perform the parameterization of f(RH), as expressed in Eq. (1). The parameterization results are displayed in Table 2.

$$f(\mathrm{RH}) = a + b \cdot \left(1 - \frac{\mathrm{RH}}{100}\right)^{-c} \quad (1)$$

The fitting parameters of f(RH) are summarized in Table 2. Large difference of the fitting parameters appears at RH below 60 %, while the parameterized f(RH) of RH ≥ 60 % presents slight variation under varying pollution conditions. At low RH, the influence of aerosol hygroscopicity on the f(RH) is indistinct, and the f(RH) could be more sensitive to the variation of the PNSD. In this sense, the difference of the fitting parameters among different pollution levels would be great. While at high RH, the variation of f(RH) is dominated by the influence coming from the aerosol hygroscopicity. Aerosol hygroscopicity is mainly determined by the mass fraction of ammonium sulfate or nitrate in the accumulation mode of the aerosol population, with the soluble mass fraction of little variation (Liu et al., 2013). Hence, the difference of this effect among varying pollution cases is not apparent. As a result, the fitting parameters would present little variation among different pollution levels.

3.4 Aerosol hygroscopicity parameter derived from the f(RH) measurements

The aerosol light scattering enhancement factor is a widely used parameter for the description of aerosol hygroscopicity. According to the single parameterized κ-Köhler theory proposed by Petters and Kreidenweis (2007), with a known mean hygroscopicity parameter, κ, the size-resolved aerosol diameter growth factors can be roughly estimated. Combining with the aerosol size distribution, the corresponding f(RH) could be calculated with the Mie model. On the contrary, the aerosol hygroscopicity parameter, κ, should be theoretically obtained with the f(RH) and PNSD measurements. It should be pointed out that the achieved κ, derived from the measured f(RH), is slightly

ACPD
14, 3459–3497, 2014

different from the size-dependent κ. The κ here represents the general mean hygroscopicity corresponding to the aerosol size distribution, reflecting the overall ability of the aerosol population taking up water, without the details of size-resolved hygroscopic growth.

Based on the method described previously (Ervens et al., 2007), a straightforward algorithm for deriving κ is proposed in this study. The main difference between the two methods is that, rather than varying the mass fraction of the insoluble compound to restrict the aerosol chemical composition in the algorithm introduced by Ervens et al., the new method is performed by changing the initial value of the assumed κ. To reduce the possible influence of observational random errors on the estimated results, all the valid f(RH) measurements in a complete humidifying cycle are used to derive the overall mean hygroscopicity parameter, κ. In particular, the κ during the 2.5 h observation period is supposed to be constant. On the assumption that all the particle size bins are of the same κ value, the size-resolved diameter growth factors at a fixed RH can be estimated according to the κ-Köhler theory.

By using the simultaneously measured mean PNSD during the entire cycle in the Mie calculation, the f(RH) corresponding to each given RH can thus be obtained with an assumed κ. With comparing the estimated f(RH) results to the in situ measured ones, a least summation of the deviations between the two f(RH) values at an individual RH should be reached at a specific κ. Consequently, the assumed κ would be regarded as the mean equivalent κ of the whole period. The algorithm procedure is illustrated in Fig. 5.

In this algorithm, the refractive index for dry aerosol particles ($\tilde{m}_{\mathrm{dry}}$) is assumed on the basis of the observations during the HaChi campaign (Ma et al., 2011), with the mean value of $\tilde{m}_{\mathrm{dry}} = 1.55 - 0.02i$. Taking into consideration of the effect of water uptake on the particle refractive index, the size-resolved refractive index for ambient aerosols after hygroscopic growth ($\tilde{m}_{\mathrm{wet}}(D_{\mathrm{wet}})$) can be obtained from the

ACPD
14, 3459–3497, 2014

volume-weighted average of the dry particle and water content:

$$\tilde{m}_{\mathrm{wet}}(D_{\mathrm{wet}}) = \frac{\left(g(\mathrm{RH}, D_{\mathrm{dry}})^3 - 1\right) \cdot \tilde{m}_{\mathrm{water}} + \tilde{m}_{\mathrm{dry}}}{g(\mathrm{RH}, D_{\mathrm{dry}})^3} \quad (2)$$

Where, D_{dry} and D_{wet} are the aerosol diameters at dry and ambient RH conditions, respectively. $g(\mathrm{RH}, D_{\mathrm{dry}})$ represents the size-resolved diameter growth factors. $\tilde{m}_{\mathrm{water}}$ is the refractive index for pure water, and it's reported to be $1.33 - 0i$.

Using the relevant parameters aforementioned, the aerosol light scattering coefficients corresponding to both dry and specific RH conditions can be derived with the Mie model. As a result, the $f(\mathrm{RH})$ at a given RH is determined, expressed as $f(\mathrm{RH})_{\mathrm{cal}}$. Accordingly, all the $f(\mathrm{RH})_{\mathrm{cal}}$ at every individual measured RH_i during the whole humidifying cycle are estimated. After that, a discriminant coefficient, F, corresponding to each assumed κ is introduced as below:

$$F = \sum_i \left(f(\mathrm{RH}_i)_{\mathrm{cal}} - f(\mathrm{RH}_i)_{\mathrm{mea}}\right)^2 \quad (3)$$

Where $f(\mathrm{RH}_i)_{\mathrm{mea}}$ stands for the in situ measured $f(\mathrm{RH})$ at a specific RH_i during the observation period. By varying the value of assumed κ, a minimum F would be achieved. Consequently, the mean equivalent κ of the entire cycle is obtained.

Figure 6 illustrates an example of the calculated κ with the described algorithm. The red circles in the left panel represent the valid $f(\mathrm{RH})$ measurements during a humidifying cycle, while the gradient colored ones denote the calculated $f(\mathrm{RH})$ corresponding to different assumed κ values. Nearly all the $f(\mathrm{RH})$ measurements are distributed in the calculation ranges. Hence, a specific κ should be definitely achieved to satisfy the requirement of minimizing the discriminant coefficient, F. The right panel of Fig. 6 just presents the results of discriminant coefficients corresponding to the varying assumed κ values shown in the left panel. It can be found that the F reaches a minimum level at $\kappa = 0.31$, indicating the mean equivalent κ of the selected cycle is 0.31.

ACPD
14, 3459–3497, 2014

With the estimation algorithm, the equivalent κ of all the effective f(RH) measurements are retrieved. Results show that, during the entire observation periods, the mean equivalent κ value varies over the range of 0.06–0.28, with a general mean value of 0.139 ± 0.050. The statistical results of the derived mean κ corresponding to different pollution cases are also summarized in Table 3.

From the statistics of the equivalent κ listed in Table 3, it indicates that differences among the equivalent κ values are commonly presented under varying pollution conditions. To be specific, in clean cases as defined beforehand, the mean value of the equivalent κ retrieved from the measured f(RH) is 0.113 ± 0.033 ; while the mean value for polluted episodes is relatively higher (0.134 ± 0.040). One possible reason can be concluded as below. Different aerosol types can lead to large variations of the aerosol hygroscopicity, and thus result in distinct variation of the f(RH). During different pollution periods, the principle chemical compositions of aerosol particles could be of great difference, hence the aerosol water uptake ability might significantly differ from each other.

3.5 An application: prediction of CCN number concentration

Combining the derived κ values, the number concentration of CCN is calculated with the f(RH) and PNSD measurements. A comparison of the predicted and in situ measured CCN number concentrations is also carried out in this section.

According to the κ-Köhler theory (Petters and Kreidenweis, 2007), with a known κ, the critical activation dry diameter, D_c, at a specific supersaturation (SS) can be theoretically derived. That is, at the given SS, particles equal or larger than D_c can be activated into CCN, while the aerosols smaller than D_c cannot be activated. Consequently, the number of activated CCN, namely N_{CCN}, at a selected SS can be calculated as

ACPD
14, 3459–3497, 2014

follows:

$$N_{CCN} = \int_{D_c}^{\infty} n(\log D) \cdot \mathrm{AR}(D) \cdot \mathrm{d}\log D \quad (4)$$

Where, D is the dry particle diameter. $n(\log D)$ stands for the in situ measured PNSD, and AR(D) represents the activation ratio, namely the number fraction of the activated aerosols to the aerosol population.

During the winter fog and haze experiment, the PNSD measurements are only in the size range of 14–736 nm, lacking the size distribution information of larger aerosols in super micron ranges. Nevertheless, the mean level of the total number concentration of particles larger than 700 nm is just 13 cm^{-3} during the 2009 HaChi winter campaign (Ma et al., 2011). As a result, without considering some special pollution episodes, e.g., dust storms, the slight influence on the N_{CCN} calculation contributed by the super micron particles could be neglected in this study.

Throughout the f(RH) observations, continuous measurements of the N_{CCN} at five specific supersaturations (0.07 %, 0.10 %, 0.20 %, 0.40 %, and 0.80 %, respectively) are simultaneously conducted. With the observed PNSDs and the real-time κ values retrieved from the f(RH) measurements, the corresponding N_{CCN} at each individual SS can be estimated with Eq. (4). Combined with the in situ measured N_{CCN}, the comparison of predicted N_{CCN} and measured values at a specific SS can be achieved. Comparison results are presented in Fig. 7.

Distinctly, at the five supersaturations, the estimation values are generally comparable with the corresponding measured N_{CCN}. At 0.07 % and 0.10 % SS, the calculated N_{CCN} are significantly lower than the in situ observations; while at SS above 0.20 %, with the increase of N_{CCN}, the predictions are evidently higher than the measured N_{CCN}. This is mainly caused by the influence of high N_{CCN} on the CCNC measurement. That is, at high N_{CCN}, the overlap of particles can result in an underestimation of the actual N_{CCN}. In addition, the limited water vapor supply in the cloud chamber of

ACPD
14, 3459–3497, 2014

the CCNC instrument could also lead to an underestimation of the measured N_{CCN} at high N_{CCN} conditions. Due to the insufficient water vapor supply, a portion should have been activated aerosols would not be activated into CCN.

To quantitatively evaluate the deviation of N_{CCN} between the predicted and measured values, a linear regression is performed to all the N_{CCN} measurements. The fitting function is as below:

$$N_{CCN,cal} = b \cdot N_{CCN,mea} \quad (5)$$

Considering the underestimation of N_{CCN} induced by high N_{CCN}, the similar influence would not appear at relatively low CCN number concentrations of $N_{CCN} < 5000\,cm^{-3}$. Consequently, the linear fitting is carried out to the following two conditions. One is aimed at all the N_{CCN} measurements. The other is just to focus on the cases of N_{CCN} below $5000\,cm^{-3}$. The corresponding fitting results at each specific SS are summarized in Table 4. Particularly, the fitting parameters displayed are the slope of the regression line, b, and the corresponding regression sum of squares, R^2, respectively.

It can be found that, apart from the relatively lower R^2 of 0.737 at 0.07 % SS, the R^2 values at the other four supersaturations are all higher than 0.8. It indicates the good correlation between the calculated N_{CCN} and measured ones. On account of the increase of N_{CCN} with the ascending SS, the fitting slope, b, of all the N_{CCN} samples also presents an evident increasing trend with the increase of SS. To be specific, b has increased from 0.62 at 0.07 % SS to 1.24 at 0.80 % SS. While in the case of $N_{CCN} < 5000\,cm^{-3}$, the slope b shows unobvious variation with the increasing SS, with generally fluctuating around 0.7. It reveals that, excluding the measurement error of the CCNC itself, the predicted N_{CCN} with the retrieved real-time κ is about 30 % lower than the measured values at a specific SS. Actually, the 30 % deviation is even lower than the measurement error stemmed from the influence of high N_{CCN}. This partially confirms that the real-time equivalent κ retrieved from the f(RH) measurements could well characterize the integral hygroscopic and activation properties of the aerosol population. Besides the real-time κ, whether the temporal averaged equivalent κ be able

ACPD
14, 3459–3497, 2014

to reliably represent the aerosol hygroscopic and activation features as well? To find a clue for it, the overall mean κ ($\kappa = 0.139$) over the whole observation period is applied in the analogous calculation of N_{CCN}, and the similar comparison and fitting of N_{CCN} between the predicted and measured results are conducted. The corresponding regression results are also displayed in Table 4.

In the case of N_{CCN} calculation with the overall mean κ, the regression slope, b, is exclusively higher than that calculated with the real-time κ at each individual SS. The corresponding R^2 values for the general mean κ cases are also significantly higher. This is more obviously presented in the fitting results for the situation of $N_{CCN} < 5000\,cm^{-3}$; the slope is more approaching 1.0, suggesting the less deviation between the estimated and measured values. This demonstrates that the prediction of N_{CCN} with the overall mean κ is more effective than that calculated with the real-time equivalent κ.

The possible reasons can be concluded as below. On one hand, previous studies have indicated that the aerosol activation property is slightly influenced by the natural variation of aerosol chemical compositions (Deng et al., 2011), while the size effect on the activation ability is dominating (Dusek et al., 2006). Consequently, the influence of the PNSD on the N_{CCN} prediction is superior to that of the aerosol hygroscopicity. Moreover, calculation error inevitably lies in the estimation of N_{CCN}. In this work, the in situ measured f(RH), PNSDs, σ_{sc} at both dry and humidified conditions, along with the RH observations, are used in the κ retrieval algorithm. All the observation parameters are of different uncertainty. It would lead to random error of the derived κ, and hence result in uncertainty for the final calculated N_{CCN}. However, with the general mean κ, the random error of κ can be reduced by the temporal averaging method to some extent. As a result, the random deviation of the predicted N_{CCN} would be decreased, thus leading to a higher correlation with the measured values.

At $N_{CCN} < 5000\,cm^{-3}$, the slope b for each specific SS is still lower than 0.9, with the minimum value of 0.61, even if calculated with the overall mean κ. The systematic deviation between the predicted and measured results could be attributed to the following accounts. Primarily, due to the lack of size-resolved aerosol hygroscopic growth

ACPD
14, 3459–3497, 2014

factors, the assumption of a constant κ to all the particle size bins is applied in the κ retrieval algorithm. This is evidently not in accordance with the actual conditions. Results show that the κ values corresponding to different particle sizes are of distinct variation (Chen et al., 2012). In addition, to the particles of a specific size, the varying aerosol chemical composition and mixing state could also result in a relatively wider probability distribution of κ (Liu et al., 2011). Therefore, the prediction of N_{CCN} based on the assumed constant κ in the whole size range would certainly possess some calculation error. Another possible explanation can be ascribed as the influence introduced by particles larger than 700 nm. With only considering the PNSDs of submicron particles, the contribution of super micron aerosols to the N_{CCN} calculation has been omitted. It might also cause uncertainty to the estimation results.

To sum up, taking into consideration of the measurement errors, along with the uncertainty of the predefined assumption in the κ retrieval process with the measured f(RH), the time averaged mean κ over a relatively long observation period is recommended to perform the N_{CCN} calculation. Alternatively, the retrieved real-time κ can be categorized into several types according to a certain classification criterion. Combined with the mean κ to different conditions, the in situ measured PNSDs can be used to predict N_{CCN}. In this sense, the retrieval algorithm for κ with the f(RH) measurements is of essential importance to the estimation of N_{CCN}. It should be mentioned that more efforts need to be taken for the improvement of f(RH) measurements, and thus achieve the goal of lower observation uncertainty but higher temporal resolution.

4 Summary and conclusions

The RH dependence of aerosol optical properties, e.g., light scattering, is a crucial input parameter for accurate estimation of the direct radiative forcing by aerosols. However, the information of aerosol hygroscopicity is always insufficiently implemented in climate models. As a result, more detailed description and parameterization of hygroscopic growth factors are greatly in need. On this account, the aerosol light scattering

ACPD
14, 3459–3497, 2014

enhancement factor, f(RH), measurements were carried out during the HaChi campaign at Wuqing site in the northern NCP. Simultaneously, ground-level PNSD, aerosol optical properties, along with the meteorological parameters, were continuously measured.

Based on the in situ observations, the variation of f(RH) corresponding to different pollution cases were discussed. The sensitivity of f(RH) to both aerosol hygroscopicity and PNSD was studied with the Mie model. The parameterization of f(RH) for different pollution cases was also performed in this work. Additionally, an improved algorithm for retrieving the aerosol hygroscopicity parameter, κ, with the f(RH) and PNSD measurements was presented. With the derived equivalent κ results, the prediction of N_{CCN} at five specific supersaturations was separately conducted by using the measured PNSDs. For quantitatively evaluation of the estimation results, comparisons of N_{CCN} between the predicted and observed values were also analyzed.

Measurements show that f(RH) dramatically increases with the ascending RH. At 80 % RH, the mean f(RH) for the entire observation period is 1.58 ± 0.22; while the corresponding mean values for clean and polluted cases are 1.46 ± 0.15 and 1.58 ± 0.19, respectively. The f(RH) for polluted cases is higher than that for clean episodes at each individual RH; with the increase of RH, the discrepancy of f(RH) is more evident. Sensitivity studies on the f(RH) influencing factors indicate that, at a specific RH, the measured f(RH) is more significantly influenced by the variation of aerosol hygroscopicity determined by its chemical compositions rather than the aerosol size distribution. A parameterization scheme of f(RH) is achieved with a polynomial segment fitting based on the statistical analysis of the f(RH) measurements. Fitting parameters among different pollution levels would present more distinct deviation at RH lower than 60 %, associated with the stronger influence of the variation of PNSD on f(RH). At RH $\geq$ 60 %, aerosol hygroscopicity is the predominant factor leading to the varying f(RH). Liu et al. (2013) have indicated that little variation is presented in the soluble mass fraction in the accumulation mode. As a consequence, it would result in unappar-

ACPD
14, 3459–3497, 2014

ent varying aerosol hygroscopicity, and hence little difference of the fitting parameters among different pollution levels.

A straightforward retrieval method of κ by using the measured f(RH) and PNSDs is proposed with the assumption that the aerosol hygroscopicity parameter is constant during a specific humidifying cycle. The derived mean equivalent κ is in the range of 0.06–0.28, with an overall mean value of 0.139 ± 0.050. The mean level of calculated equivalent κ for clean cases (0.113 ± 0.033) is much lower than that of pollution episodes (0.134 ± 0.040).

As an application, the calculated κ is used to predict CCN number concentration. The comparison between the calculated CCN number concentration and in situ measured results reveals a good agreement at each specific supersaturation, especially at high supersaturation conditions. This indicates the proposed κ retrieval algorithm with the f(RH) measurements is reasonable and robust.

Acknowledgements. This work is supported by the National 973 project of China (2011CB403402), the National Natural Science Foundation of China under Grant no. 41375134, and the Beijing Natural Science Foundation (8131003).

References

Bohren, C. F. and Huffman, D. R.:Absorption and Scattering of Light by Small Particles, John Wiley, Hoboken, 477–482, 1983.

Carrico, C., Rood, M., and Ogren, J.: Aerosol light scattering properties at Cape Grim, Tasmania, during the first Aerosol Characterization Experiment (ACE 1), J. Geophys. Res., 103, 16565–16574, doi:10.1029/98JD00685, 1998.

Carrico, C., Rood, M., Ogren, J., Neusüß, C., Wiedensohler, A., and Heintzenberg, J.: Aerosol optical properties at Sagres, Portugal, during ACE-2, Tellus B, 52, 694–715, doi:10.1034/j.1600-0889.2000.00049.x, 2000.

Carrico, C., Kus, P., Rood, M., Quinn, P., and Bates, T.: Mixtures of pollution, dust, sea salt, and volcanic aerosol during ACE-Asia: radiative properties as a function of relative humidity, J. Geophys. Res., 108, 8650, doi:10.1029/2003JD003405, 2003.

ACPD
14, 3459–3497, 2014

Charlson, R. J., Schwartz, S. E., Hales, J. M., Cess, R. D., Coakley Jr., J. A., Hansen, J. E., and Hofmann, D. J.: Climate forcing by anthropogenic aerosols, Science, 255, 423–430, 1992.

Chen, J., Zhao, C. S., Ma, N., Liu, P. F., Göbel, T., Hallbauer, E., Deng, Z. Z., Ran, L., Xu, W. Y., Liang, Z., Liu, H. J., Yan, P., Zhou, X. J., and Wiedensohler, A.: A parameterization of low visibilities for hazy days in the North China Plain, Atmos. Chem. Phys., 12, 4935–4950, doi:10.5194/acp-12-4935-2012, 2012.

Cheng, Y. F., Eichler, H., Wiedensohler, A., Heintzenberg, J., Zhang, Y. H., Hu, M., Herrmann, H., Zeng, L. M., Liu, S., Gnauk, T., Brüggemann, E., and He, L. Y.: Mixing state of elemental carbon and non-light-absorbing aerosol components derived from in situ particle optical properties at Xinken in Pearl River Delta of China, J. Geophys. Res., 111, D20204, doi:10.1029/2005JD006929, 2006.

Cheng, Y. F., Wiedensohler, A., Eichler, H., Su, H., Gnauk, T., Brüggemann, E., Herrmann, H., Heintzenberg, J., Slanina, J., Tuch, T., Hu, M., and Zhang, Y. H.: Aerosol optical properties and related chemical apportionment at Xinken in Pearl River Delta of China, Atmos. Environ., 42, 6351–6372, 2008.

Covert, D. S., Charlson, R. J., and Ahlquist, N. C.: A study of the relationship of chemical composition and humidity to light scattering by aerosols, J. Appl. Meteorol., 11, 968–976, 1972.

Deng, Z. Z., Zhao, C. S., Ma, N., Liu, P. F., Ran, L., Xu, W. Y., Chen, J., Liang, Z., Liang, S., Huang, M. Y., Ma, X. C., Zhang, Q., Quan, J. N., Yan, P., Henning, S., Mildenberger, K., Sommerhage, E., Schäfer, M., Stratmann, F., and Wiedensohler, A.: Size-resolved and bulk activation properties of aerosols in the North China Plain, Atmos. Chem. Phys., 11, 3835–3846, doi:10.5194/acp-11-3835-2011, 2011.

Dusek, U., Frank, G. P., Hildebrandt, L., Curtius, J., Schneider, J., Walter, S., Chand, D., Drewnick, F., Hings, S., Jung, D., Borrmann, S., and Andreae, M. O.: Size matters more than chemistry for cloud-nucleating ability of aerosol particles, Science, 312, 1375–1378, 2006.

Ervens, B., Cubison, M., Andrews, E., Feingold, G., Ogren, J. A., Jimenez, J. L., DeCarlo, P., and Nenes, A.: Prediction of cloud condensation nucleus number concentration using measurements of aerosol size distributions and composition and light scattering enhancement due to humidity, J. Geophys. Res., 112, D10S32, doi:10.1029/2006JD007426, 2007.

ACPD
14, 3459–3497, 2014

Fierz-Schmidhauser, R., Zieger, P., Gysel, M., Kammermann, L., DeCarlo, P. F., Baltensperger, U., and Weingartner, E.: Measured and predicted aerosol light scattering enhancement factors at the high alpine site Jungfraujoch, Atmos. Chem. Phys., 10, 2319–2333, doi:10.5194/acp-10-2319-2010, 2010a.

Fierz-Schmidhauser, R., Zieger, P., Vaishya, A., Monahan, C., Bialek, J., O'Dowd, C. D., Jennings, S. G., Baltensperger, U., and Weingartner, E.: Light scattering enhancement factors in the marine boundary layer (Mace Head, Ireland), J. Geophys. Res., 115, D20204, doi:10.1029/2009jd013755, 2010b.

Fierz-Schmidhauser, R., Zieger, P., Wehrle, G., Jefferson, A., Ogren, J. A., Baltensperger, U., and Weingartner, E.: Measurement of relative humidity dependent light scattering of aerosols, Atmos. Meas. Tech., 3, 39–50, doi:10.5194/amt-3-39-2010, 2010c.

Fitzgerald, J., Hoppel, W., and Vietti, M.: The size and scattering coefficient of urban aerosol particles at Washington, DC as a function of relative humidity, J. Atmos. Sci., 39, 1838–1852, 1982.

Gasso, S., Hegg, D., Covert, D., Collins, D., Noone, K., Öström, E., Schmid, B., Russell, P., Livingston, J., Durkee, P., and Jonsson, H.: Influence of humidity on the aerosol scattering coefficient and its effect on the upwelling radiance during ACE-2, Tellus B, 52, 546–567, 2000.

Hegg, D. A., Covert, D. S., Crahan, K., and Jonssen, H.: The dependence of aerosol light-scattering on RH over the Pacific Ocean, Geophys. Res. Lett., 29, 1219, doi:10.1029/2001GL014495, 2002

IPCC: Climate Change 2007 – The Physical Science Basis, edited by: Solomon, S., Cambridge Univ. Press, New York, 2007.

Kim, J., Yoon, S.-C., Jefferson, A., and Kim, S.-W.: Aerosol hygroscopic properties during Asian dust, pollution, and biomass burning episodes at Gosan, Korea, in April 2001, Atmos. Environ., 40, 1550–1560, 2006.

Kotchenruther, R. and Hobbs, P.: Humidification factors of aerosols from biomass burning in Brazil, J. Geophys. Res., 103, 32081–32089, doi:10.1029/98JD00340, 1998.

Kotchenruther, R. A., Hobbs, P. V., and Hegg, D. A.: Humidification factors for atmospheric aerosols off the mid-Atlantic coast of the United States, J. Geophys. Res., 104, 2239–2251, 1999.

Lance, S., Medina, J., Smith, J. N., and Nenes, A.: Mapping the operation of the dmt continuous flow CCN counter, Aerosol Sci. Tech., 40, 242–254, 2006.

ACPD
14, 3459–3497, 2014

Lesins, G., Chylek, P., and Lohman, U.: A study of internal and external mixing scenarios and its effect on aerosol optical properties and direct radiative forcing, J. Geophys. Res., 107, 4094, doi:10.1029/2001JD000973, 2002.

Li-Jones, X., Maring, H., and Prospero, J.: Effect of relative humidity on light scattering by mineral dust aerosol as measured in the marine boundary layer over the tropical Atlantic Ocean, J. Geophys. Res., 103, 31113–31121, doi:10.1029/98JD01800, 1998.

Liu, H. J., Zhao, C. S., Nekat, B., Ma, N., Wiedensohler, A., van Pinxteren, D., Spindler, G., Müller, K., and Herrmann, H.: Aerosol hygroscopicity derived from size-segregated chemical composition and its parameterization in the North China Plain, Atmos. Chem. Phys. Discuss., 13, 20885–20922, doi:10.5194/acpd-13-20885-2013, 2013.

Liu, P. F., Zhao, C. S., Göbel, T., Hallbauer, E., Nowak, A., Ran, L., Xu, W. Y., Deng, Z. Z., Ma, N., Mildenberger, K., Henning, S., Stratmann, F., and Wiedensohler, A.: Hygroscopic properties of aerosol particles at high relative humidity and their diurnal variations in the North China Plain, Atmos. Chem. Phys., 11, 3479–3494, doi:10.5194/acp-11-3479-2011, 2011.

Ma, N., Zhao, C. S., Nowak, A., Müller, T., Pfeifer, S., Cheng, Y. F., Deng, Z. Z., Liu, P. F., Xu, W. Y., Ran, L., Yan, P., Göbel, T., Hallbauer, E., Mildenberger, K., Henning, S., Yu, J., Chen, L. L., Zhou, X. J., Stratmann, F., and Wiedensohler, A.: Aerosol optical properties in the North China Plain during HaChi campaign: an in-situ optical closure study, Atmos. Chem. Phys., 11, 5959–5973, doi:10.5194/acp-11-5959-2011, 2011.

Malm, W. C. and Day, D. E.: Estimates of aerosol species scattering characteristics as a function of relative humidity, Atmos. Environ., 35, 2845–2860, doi:10.1016/s1352-2310(01)00077-2, 2001.

Malm, W. C., Day, D. E., Kreidenweis, S. M., Collett, J. L., and Lee, T.: Humidity-dependent optical properties of fine particles during the big bend regional aerosol and visibility observational study, J. Geophys. Res., 108, 4279, doi:10.1029/2002jd002998, 2003.

Massling, A., Stock, M., Wehner, B., Wu, Z. J., Hu, M., Brüggemann, E., Gnauk, T., Herrmann, H., and Wiedensohler, A.: Size segregated water uptake of the urban submicrometer aerosol in Beijing, Atmos. Environ., 43, 1578–1589, 2009.

McInnes, L., Bergin, M., Ogren, J., and Schwartz, S.: Apportionment of light scattering and hygroscopic growth to aerosol composition, Geophys. Res. Lett., 25, 513–516, doi:10.1029/98GL00127, 1998.

Meier, J., Wehner, B., Massling, A., Birmili, W., Nowak, A., Gnauk, T., Brüggemann, E., Herrmann, H., Min, H., and Wiedensohler, A.: Hygroscopic growth of urban aerosol particles

ACPD
14, 3459–3497, 2014

in Beijing (China) during wintertime: a comparison of three experimental methods, Atmos. Chem. Phys., 9, 6865–6880, doi:10.5194/acp-9-6865-2009, 2009.
Mie, G.: Beiträge zur optic trüber Medien speziell kolloidaler Metallösungen, Ann. Phys., 25, 377–445, 1908.
Nessler, R., Weingartner, E., and Baltensperger, U.: Adaptation of dry nephelometer measurements to ambient conditions at the Jungfraujoch, Environ. Sci. Technol., 39, 2219–2228, 2005.
Pan, X. L., Yan, P., Tang, J., Ma, J. Z., Wang, Z. F., Gbaguidi, A., and Sun, Y. L.: Observational study of influence of aerosol hygroscopic growth on scattering coefficient over rural area near Beijing mega-city, Atmos. Chem. Phys., 9, 7519–7530, doi:10.5194/acp-9-7519-2009, 2009.
Petters, M. D. and Kreidenweis, S. M.: A single parameter representation of hygroscopic growth and cloud condensation nucleus activity, Atmos. Chem. Phys., 7, 1961–1971, doi:10.5194/acp-7-1961-2007, 2007.
Pilat, M. J. and Charlson, R. J.: Theoretical and optical studies of humidity effects on the size distribution of hygroscopic aerosol, J. Rech. Atmos., 1, 165–170, 1966.
Ran, L., Zhao, C. S., Xu, W. Y., Lu, X. Q., Han, M., Lin, W. L., Yan, P., Xu, X. B., Deng, Z. Z., Ma, N., Liu, P. F., Yu, J., Liang, W. D., and Chen, L. L.: VOC reactivity and its effect on ozone production during the HaChi summer campaign, Atmos. Chem. Phys., 11, 4657–4667, doi:10.5194/acp-11-4657-2011, 2011.
Randriamiarisoa, H., Chazette, P., Couvert, P., Sanak, J., and Mégie, G.: Relative humidity impact on aerosol parameters in a Paris suburban area, Atmos. Chem. Phys., 6, 1389–1407, doi:10.5194/acp-6-1389-2006, 2006.
Roberts, G. C. and Nenes, A.: A continuous-flow streamwise thermal-gradient CCN chamber for atmospheric measurements, Aerosol Sci. Tech., 39, 206–221, 2005.
Schwartz, S.: The Whitehouse Effect–Shortwave radiative forcing of climate by anthropogenic aerosols: an overview, J. Aerosol Sci., 27, 359–382, 1996.
Seinfeld, J. H. and Pandis, S. N.: Atmospheric Chemistry and Physics, John Wiley & Sons, Inc., New York, 1998.
Sheridan, P., Delene, D., and Ogren, J.: Four years of continuous surface aerosol measurements from the department of energy's atmospheric radiation measurement program southern great plains cloud and radiation testbed site, J. Geophys. Res., 106, 20735–20747, 2001.
Wang, W., Rood, M., Carrico, C., Covert, D., Quinn, P., and Bates, T.: Aerosol optical properties along the northeast coast of North America during the New England air quality study –

ACPD
14, 3459–3497, 2014

intercontinental transport and chemical transformation 2004 campaign and the influence of aerosol composition, J. Geophys. Res., 112, D10S23, doi:10.1029/2006JD007579, 2007.
Yan, P., Pan, X., Tang, J., Zhou, X., Zhang, R., and Zeng, L.: Hygroscopic growth of aerosol scattering coefficient: A comparative analysis between urban and suburban sites at winter in Beijing, Particuology, 7, 52–60, 2009.
Yuan, C.-S., Lee, C.-G., Liu, S.-H., Chang, J.-C., Yuan, C., and Yang, H.-Y.: Correlation of atmospheric visibility with chemical composition of Kaohsiung aerosols, Atmos. Res., 82, 663–679, 2006.
Zieger, P., Fierz-Schmidhauser, R., Gysel, M., Ström, J., Henne, S., Yttri, K. E., Baltensperger, U., and Weingartner, E.: Effects of relative humidity on aerosol light scattering in the Arctic, Atmos. Chem. Phys., 10, 3875–3890, doi:10.5194/acp-10-3875-2010, 2010.
Zieger, P., Weingartner, E., Henzing, J., Moerman, M., de Leeuw, G., Mikkilä, J., Ehn, M., Petäjä, T., Clémer, K., van Roozendael, M., Yilmaz, S., Frieß, U., Irie, H., Wagner, T., Shaiganfar, R., Beirle, S., Apituley, A., Wilson, K., and Baltensperger, U.: Comparison of ambient aerosol extinction coefficients obtained from in-situ, MAX-DOAS and LIDAR measurements at Cabauw, Atmos. Chem. Phys., 11, 2603–2624, doi:10.5194/acp-11-2603-2011, 2011.
Zieger, P., Kienast-Sjögren, E., Starace, M., von Bismarck, J., Bukowiecki, N., Baltensperger, U., Wienhold, F. G., Peter, T., Ruhtz, T., Collaud Coen, M., Vuilleumier, L., Maier, O., Emili, E., Popp, C., and Weingartner, E.: Spatial variation of aerosol optical properties around the high-alpine site Jungfraujoch (3580 m a.s.l.), Atmos. Chem. Phys., 12, 7231–7249, doi:10.5194/acp-12-7231-2012, 2012.
Zieger, P., Fierz-Schmidhauser, R., Weingartner, E., and Baltensperger, U.: Effects of relative humidity on aerosol light scattering: results from different European sites, Atmos. Chem. Phys., 13, 10609–10631, doi:10.5194/acp-13-10609-2013, 2013.

ACPD
14, 3459–3497, 2014

Table 1. The measured f(RH), with the mean value ± standard deviation (σ), at given RHs under different pollution levels.

RH	f(RH)		
	Average	Clean	Polluted
50 % ± 1 %	1.08 ± 0.09	1.03 ± 0.06	1.12 ± 0.08
55 % ± 1 %	1.12 ± 0.09	1.04 ± 0.07	1.16 ± 0.06
60 % ± 1 %	1.19 ± 0.13	1.09 ± 0.06	1.19 ± 0.11
65 % ± 1 %	1.21 ± 0.15	1.12 ± 0.10	1.29 ± 0.13
70 % ± 1 %	1.36 ± 0.15	1.20 ± 0.09	1.34 ± 0.11
75 % ± 1 %	1.40 ± 0.17	1.34 ± 0.15	1.48 ± 0.14
80 % ± 1 %	1.58 ± 0.22	1.46 ± 0.15	1.58 ± 0.19
85 % ± 1 %	1.66 ± 0.23	1.57 ± 0.16	1.70 ± 0.24
90 % ± 1 %	1.90 ± 0.27	1.71 ± 0.26	1.93 ± 0.21

ACPD
14, 3459–3497, 2014

Table 2. The polynomial segment fitting parameter results of f(RH) for different pollution cases.

RH Ranges	Fitting parameters	Average (R^2 = 0.82)	Clean (R^2 = 0.76)	Polluted (R^2 = 0.85)
RH < 60 %	a	1.030 ± 0.012	1.005 ± 0.008	1.042 ± 0.019
	b	(4.035 ± 4.107) × 10^{-3}	(1.790 ± 0.577) × 10^{-3}	(6.108 ± 7.082) × 10^{-3}
	c	3.935 ± 1.105	4.0	3.684 ± 1.238
RH ≥ 60 %	a	−3.0 ± 1.584	−3.0 ± 6.438	−3.0 ± 1.898
	b	3.809 ± 1.557	3.768 ± 6.362	3.872 ± 1.865
	c	0.107 ± 0.036	0.097 ± 0.140	0.105 ± 0.042

ACPD
14, 3459–3497, 2014

Table 3. Statistical results of the mean hygroscopicity parameter, κ, derived from f(RH) observations (n denotes the sample size corresponding to each case).

Statistics		κ		
		Average (n = 117)	Clean (n = 24)	Polluted (n = 50)
Mean		0.139	0.113	0.134
Std		0.050	0.033	0.040
Min		0.06	0.06	0.06
Max		0.28	0.16	0.28
Percentile	5	0.07	0.06	0.09
	10	0.09	0.07	0.09
	25	0.10	0.09	0.10
	50	0.13	0.11	0.14
	75	0.17	0.15	0.15
	90	0.21	0.15	0.17
	95	0.25	0.16	0.21

ACPD
14, 3459–3497, 2014

Table 4. Fitting parameters of the linear regression results in Fig. 7.

	Real-time κ				Overall mean κ			
	All		$N_{CCN} < 5000\,cm^{-3}$		All		$N_{CCN} < 5000\,cm^{-3}$	
SS	b	R^2	b	R^2	b	R^2	b	R^2
0.07 %	0.620	0.737	0.600	0.750	0.627	0.821	0.610	0.837
0.10 %	0.877	0.835	0.755	0.876	0.888	0.896	0.840	0.902
0.20 %	1.04	0.841	0.662	0.818	1.06	0.881	0.686	0.902
0.40 %	1.05	0.874	0.561	0.803	1.08	0.901	0.678	0.878
0.80 %	1.24	0.901	0.771	0.510	1.26	0.913	0.891	0.503

ACPD
14, 3459–3497, 2014

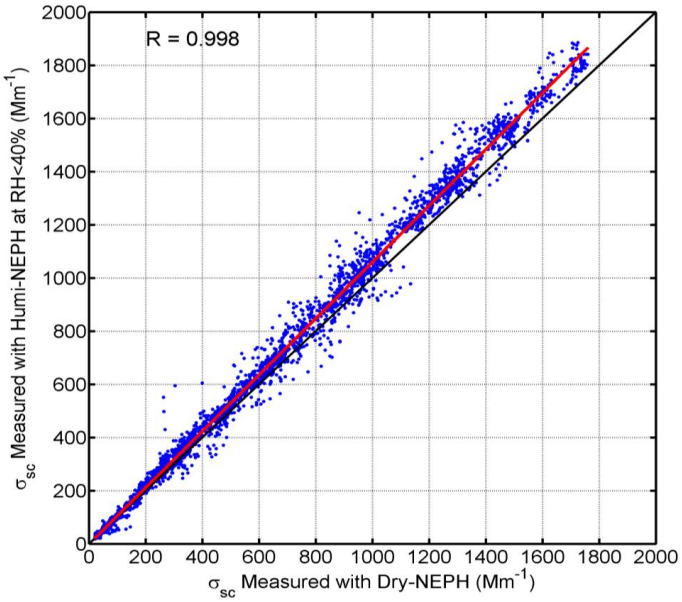

Fig. 1. Comparison of dry σ_{sc} between that measured with the humidified and reference nephelometers at dry conditions (RH < 40 %).

ACPD
14, 3459–3497, 2014

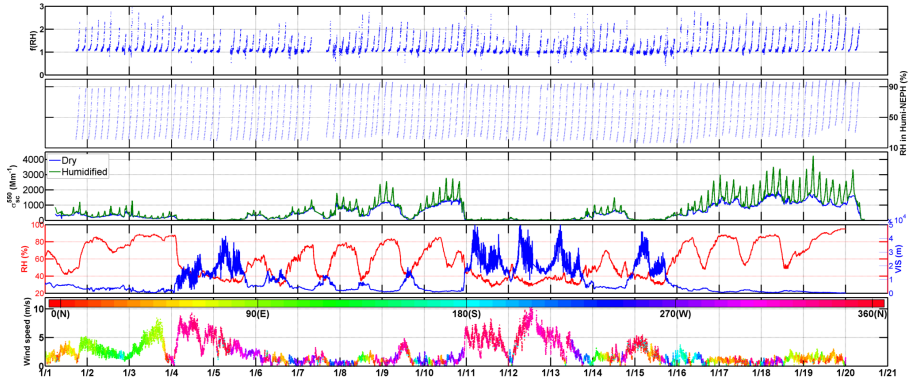

Fig. 2. Time series of measured aerosol optical and meteorological parameters. Top-down subplots orderly display the f(RH) measurements at elevated RH, the corresponding RHs inside the Humi-NEPH in ascending RH periods, aerosol light scattering coefficients at 550 nm wavelength (σ_{sc}^{550}) at both dry and humidified conditions, every minute RH and visibility (VIS) records, as well as the wind parameter.

ACPD
14, 3459–3497, 2014

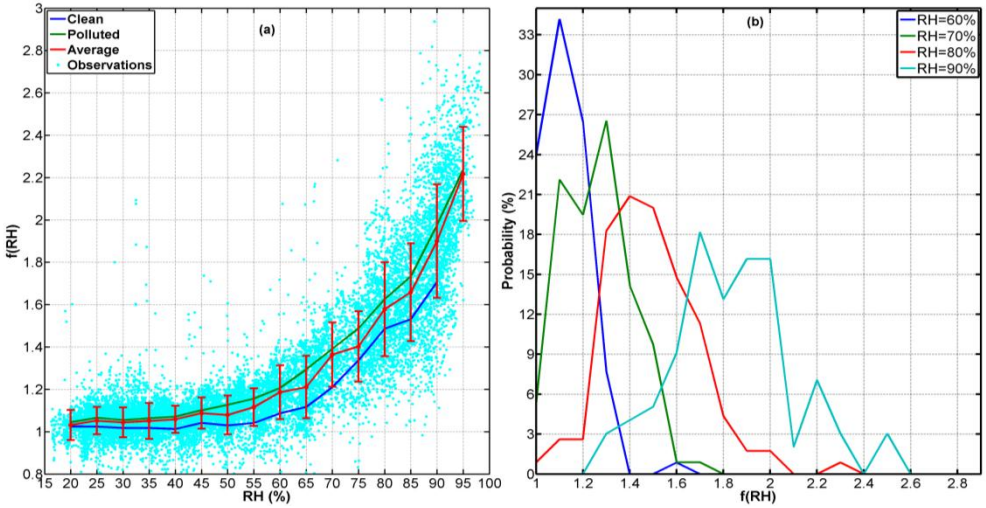

Fig. 3. (a) The mean f(RH) under clean, average (mean $\pm 1\sigma$), and polluted conditions. The scattered dots represent the in situ observational results, and lines denote the mean f(RH) values corresponding to different pollution cases. **(b)** Probability distributions (PDF) of f(RH) at four specific RHs (RH = 60 %, 70 %, 80 %, and 90 %, respectively).

ACPD
14, 3459–3497, 2014

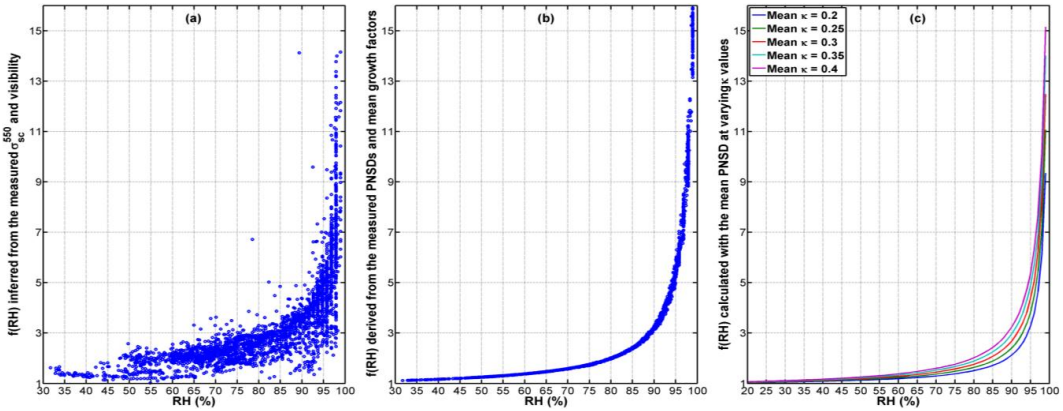

Fig. 4. Sensitivity tests of **(b)** the PNSD and **(c)** hygroscopicity parameter κ to f(RH) based on in situ measured PNSDs and aerosol hygroscopic growth factors during the HaChi summer campaign. The subplot **(a)** represented the measured f(RH) derived from the in situ observations.

ACPD
14, 3459–3497, 2014

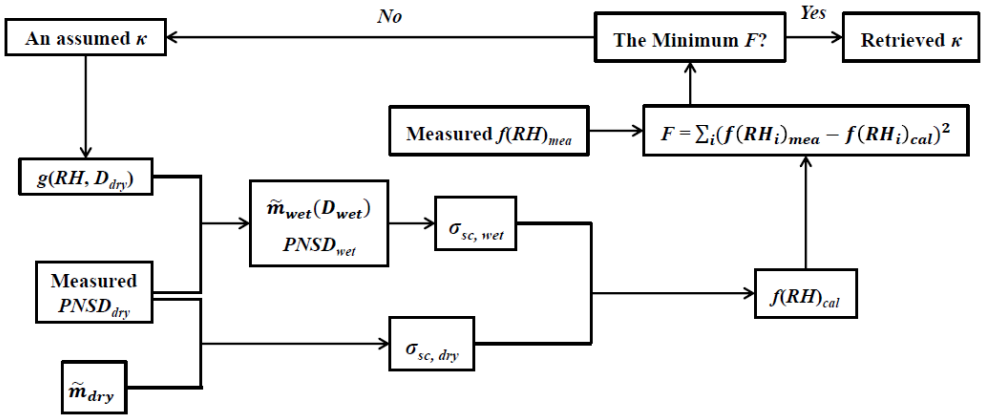

Fig. 5. The flow chart of the retrieval algorithm for aerosol hygroscopicity parameter, κ.

ACPD
14, 3459–3497, 2014

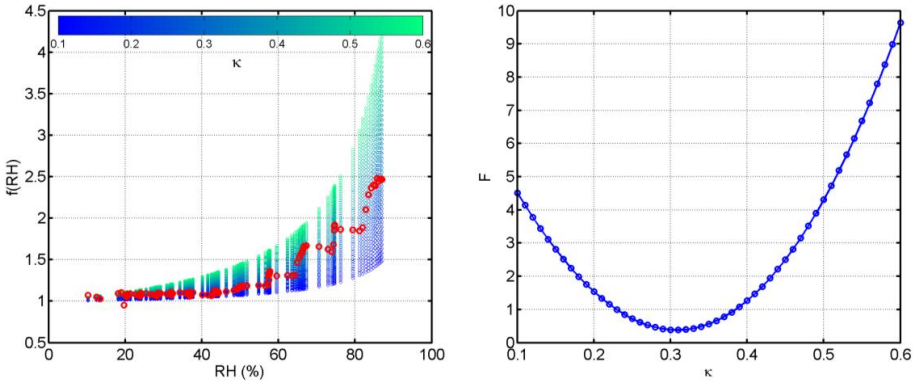

Fig. 6. One case of the calculated κ. In the left panel, the red circles stand for the valid f(RH) observations during a humidifying cycle, while the gradient colored ones represent the corresponding f(RH) calculated with an assumed specific κ. The right panel shows the discriminant coefficient, F, corresponding to each assumed κ.

ACPD
14, 3459–3497, 2014

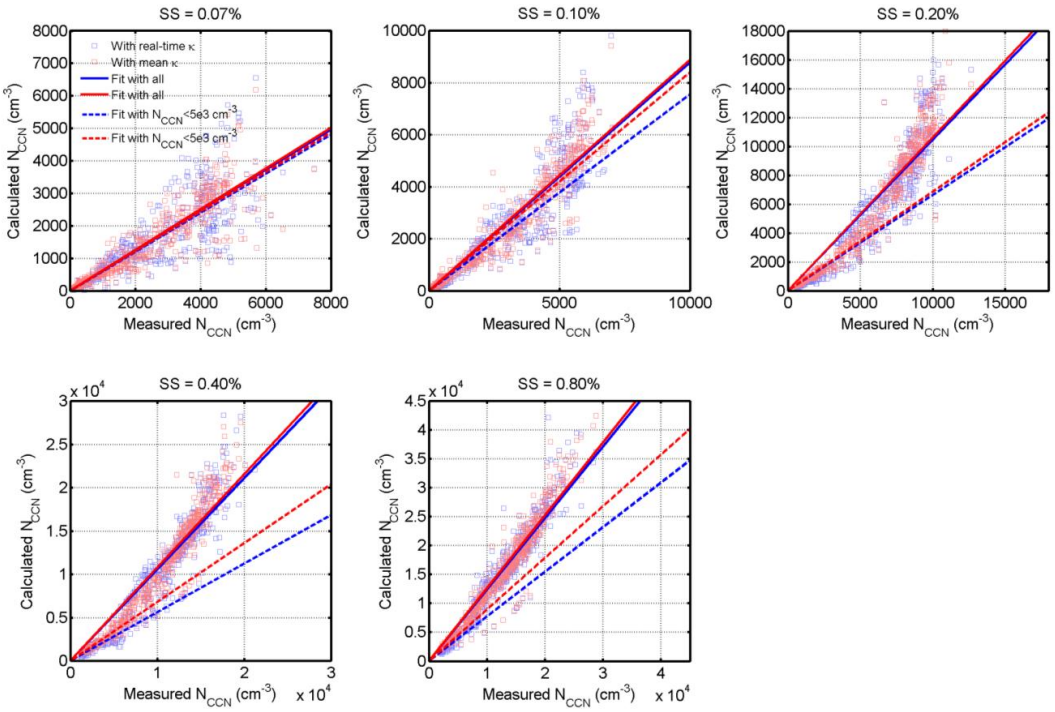

Fig. 7. Comparison between in situ measured N_{CCN} and calculated N_{CCN} at five specific supersaturations. Blue squares represent the estimated N_{CCN} with the real-time κ, while the red ones denote the estimation results with the overall mean κ during the entire f(RH) measurements. The blue and red solid lines stand for the fitting results of all the N_{CCN} samples corresponding to the two kinds of κ, respectively; while the blue and red dashed lines are the fitting results in the case of measured $N_{CCN} < 5000\,\mathrm{cm}^{-3}$.

ACPD
14, 3459–3497, 2014